

13.1

Oxide/InAs(001) interface passivation with fluorine

© M.S. Aksenov^{1,2}, V.A. Golyashov^{1,2}, O.E. Tereshchenko^{1,2}

¹ Rzhanov Institute of Semiconductor Physics, Siberian Branch, Russian Academy of Sciences, Novosibirsk, Russia

² Novosibirsk State University, Novosibirsk, Russia

E-mail: aksenov@isp.nsc.ru

Received November 7, 2022

Revised December 15, 2022

Accepted December 20, 2022

It is shown that fluorine-containing anodic layers on the *n*-InAs(001) surface, in contrast to fluorine-free anodic layers, form an interface with unpinned Fermi level, the density of states on which near the midgap is about $10^{11} \text{ eV}^{-1} \cdot \text{cm}^{-2}$ (78 K). The study of the chemical composition showed that the decrease in the density of states is associated with the formation of indium and arsenic oxyfluorides near the interface.

Keywords: InAs, MIS structure, fluorine, anodic layer, interface states.

DOI: 10.21883/TPL.2023.03.55672.19413

Techniques of fabrication of planar multi-gate field-effect transistors (FETs) with InAs channel layers have progressed rapidly in the recent decade [1]. The interest in these devices stems in part from experiments on integrating narrow-gap A_3B_5 (InAs, InGaAs, InSb, GaSb) semiconductor channels with the CMOS process [2]. Since the linear dimensions (diameter, width) of channels in modern multi-gate transistors are on the order of tens of nanometers, the quality of the gate insulator/semiconductor interface, which is governed by the density of electronic states in the semiconductor bandgap (D_{it}), exerts a decisive influence on the speed performance of a transistor. High D_{it} values at the insulator/ A_3B_5 interface are the primary factor limiting the application of transistors and are normally associated, in the case of *ex situ* fabrication, with the native semiconductor oxide layer [3]. The most widespread current method of formation of these interfaces is the atomic layer deposition (ALD) of dielectrics with a high permittivity (high- k) preceded by the removal of native oxide and other chemical treatment procedures aimed at passivation of the semiconductor surface. Although the amount of semiconductor oxides decreases in the first ALD cycles under the influence of the main precursor („self-cleaning“ effect) [4], it is rather hard to remove them completely [5], not least because of the possible reoxidation of a semiconductor by an oxidizer [6].

Passivation of oxygen-related electronic states by halogens, which has been demonstrated earlier for InAs(111)A and fluorine [7], is one of the ways to reduce D_{it} . However, this effect for the most widespread InAs material with the (001) orientation has not been examined. Owing to the specifics of the local structure of a transition layer at the interface with an insulator [7,9], the InAs surface orientation may have a significant influence on D_{it} [8].

In the present study, we reveal the influence of fluorine on the electronic properties of the anodic (native)

oxide/InAs(001) interface by analyzing the capacitance–voltage (C-V) curves measured at a temperature of 78 K.

Bulk *epi-ready n*-InAs(001) substrates doped with sulfur and produced by Pam-Xiamen (China) were used in experiments. According to the specifications, the dopant impurity density was $(4-6) \cdot 10^{17} \text{ cm}^{-3}$.

All samples were deoiled in a solution of monoethanolamine with hydrogen peroxide, immersed into a HCl : H₂O = 1 : 10 mixture for 60 s to remove the residual oxide layer, and introduced into the vacuum chamber. Anodic oxide (AO) layers and fluorine-containing anodic oxide (FAO) layers with a thickness of 5–15 nm were formed in low-energy DC plasma of Ar : O₂ = 4 : 1 and Ar : O₂ : CF₄ = 7.7 : 2 : 0.3 gas mixtures, respectively, under a pressure of 2 Torr [10].

Round gate contacts with an area of $2 \cdot 10^{-3} \text{ cm}^2$ were fabricated by deposition of Ti (20 nm)/Au (200 nm) metal layers through a mask. An Ohmic contact to the back surface of samples was formed by deposition of a 400-nm-thick In layer.

The C-V curves of prepared metal–insulator–semiconductor (MIS) structures were measured using a Keysight B1500A semiconductor parameter analyzer and a thermostabilized probe station at a temperature of 78 K in the dark.

The method of calculation of theoretical C-V curves with an assumed lack of interface states was detailed in [11]. The Fermi–Dirac statistics was used in the calculations; nonparabolicity of the dispersion law and quantization of the electron energy in the space charge region were taken into account. The parameters of InAs used in the calculations were taken from [12]. The work function of Ti and the permittivity of anodic layers were assumed to be equal to 4.2 eV and 6, respectively.

The chemical composition of the FAO/InAs(001) interface was examined by X-ray photoelectron spectroscopy (XPS) using a SPECS GmbH ProvenX-ARPES system fitted

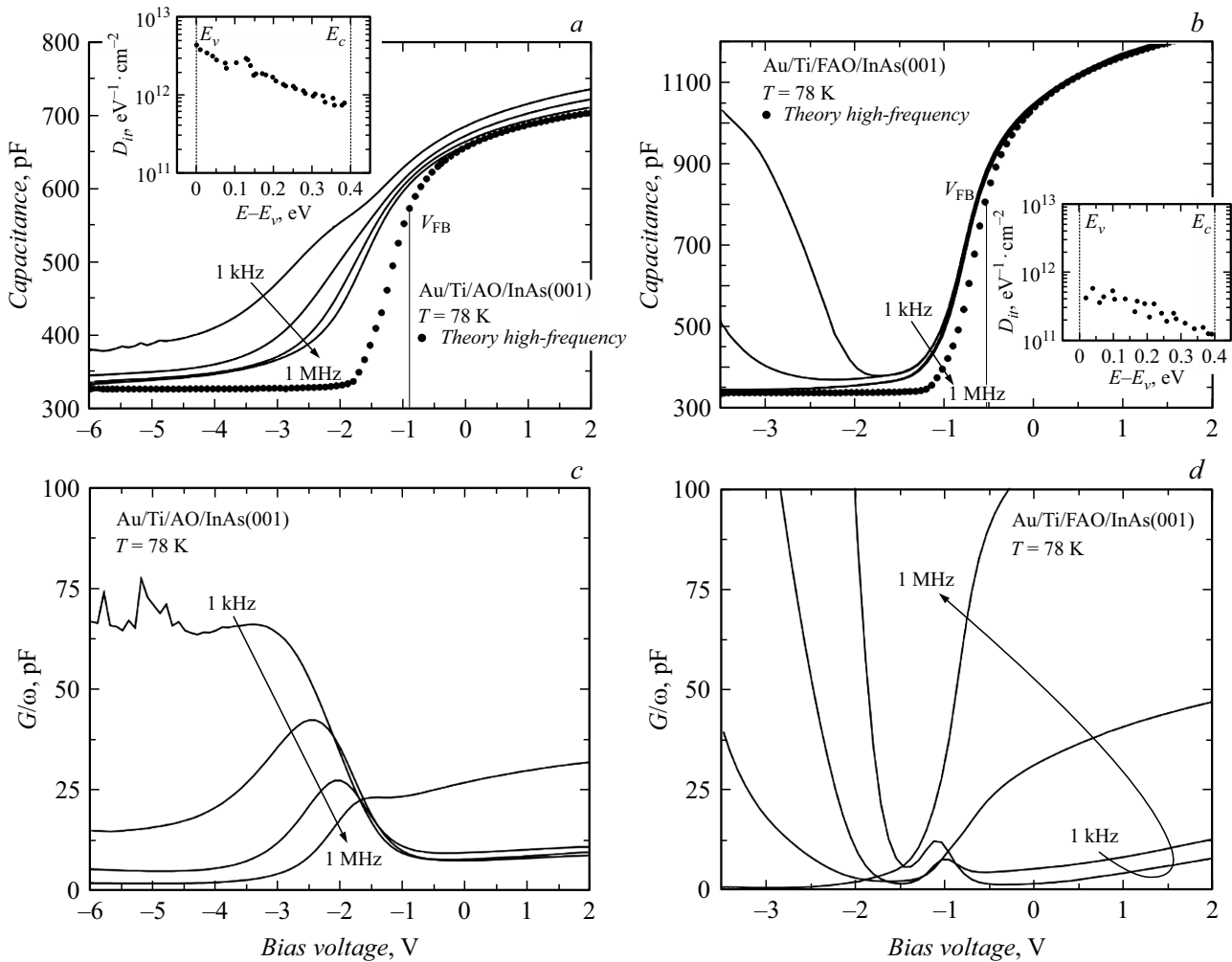


Figure 1. Frequency (1 kHz, 10 kHz, 100 kHz, 1 MHz) dependences of C-V curves (a,b) and $G/\omega-V$ (c,d) of Au/Ti/AO(~ 13 nm)/ n -InAs(001) (a,c) and Au/Ti/FAO(~ 7 nm)/ n -InAs(001) (b,d) MIS structures measured at a temperature of 78 K. The corresponding distributions of D_{it} (78 K) in the bandgap of InAs are shown in the insets.

with an ASTRAIOS 190 electron energy analyzer and a 2D-CMOS electron detector. Focused monochromatic AlK_{α} radiation ($h\nu = 1486.7$ eV, 150 W) was the source of excitation. XPS spectra were recorded under normal radiation incidence with a constant pass energy of 30 eV and an energy resolution of ≤ 0.6 eV. The spectrometer energy scale was calibrated by positioning the measured binding energy of the Ag $3d_{5/2}$ line, which was 368.22 ± 0.05 eV, relative to the Fermi energy.

Figure 1 presents the dependences of typical C-V curves measured at variable-signal frequencies of 1 kHz, 10 kHz, 100 kHz, and 1 MHz at a temperature of 78 K for MIS structures with thin (5–15 nm) AO (a) and FAO (b) layers. The corresponding ideal CVCs calculated for nominal values of the dopant impurity density are shown by dots in the same figure.

Typical C-V curves of structures with fluorine-free AO layers (Fig. 1,a) feature a significant frequency dispersion in enrichment (from 0 to +2V), which is attributable to the influence of border traps [13], and in depletion

(from -3 to -0.5 V), which is due to the charge exchange with interface (surface) states [7,13]. The C-V curves for a frequency of 1 kHz at bias voltages ranging from -6 to -4 V runs way above the theoretical value in inversion. This is attributable to pinning of the Fermi level below the midgap. The distribution of D_{it} (78 K) in the bandgap of InAs determined using the Terman method [14] (by comparing the slopes of experimental and theoretical C-V curves) is presented in the inset of Fig. 1,a. The value of D_{it} near the midgap (E_g) is $\sim 2 \cdot 10^{12}$ $eV^{-1} \cdot cm^{-2}$ (78 K). Frequency dependences of normalized conductance $G/\omega-V$ in Fig. 1,c feature characteristic peaks related to the charge exchange with interface states. The estimation of the upper D_{it} limit by the conductance technique [15] yields close ($\sim 8 \cdot 10^{11}$ $eV^{-1} \cdot cm^{-2}$) values near the midgap.

The introduction of fluorine-containing CF_4 into the gas mixture for anodic oxidation leads to significant changes in the behavior of frequency dependences of C-V curves. Typical C-V curves of structures with FAO layers (Fig. 1,b) have near-zero frequency dispersion in enrichment (from 0

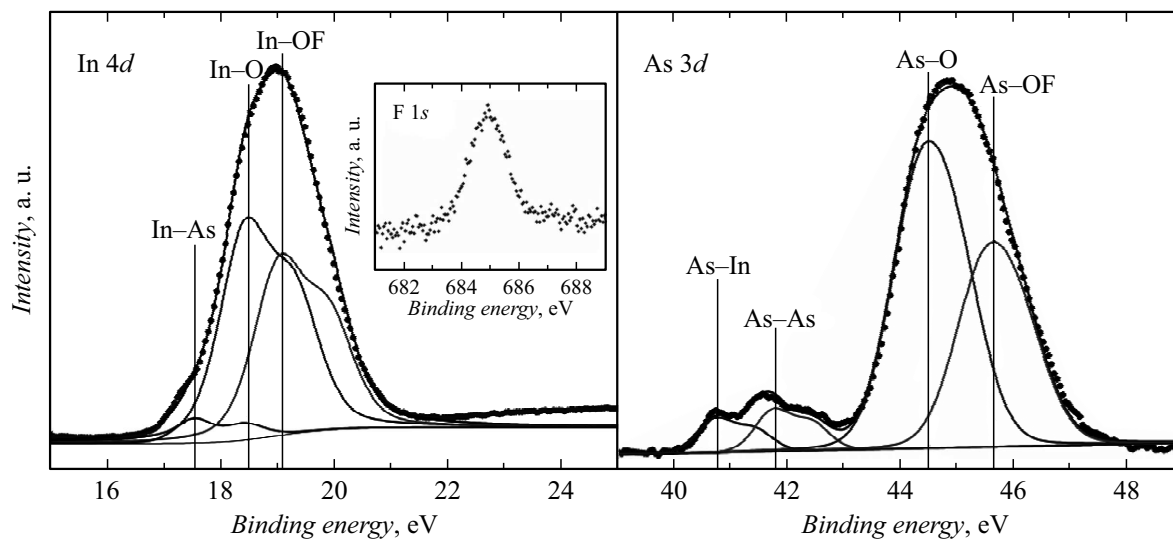


Figure 2. XPS spectra of In 4*d*, As 3*d*, and F 1*s* (inset) lines on the initial FAO surface with a thickness of 7–8 nm.

to +1.5 V) and depletion (from –1 to 0 V). This is attributable to a low density of border traps and interface states. The C-V curve for 1 kHz has a classical low-frequency shape with the capacitance increasing (minority carrier response) in strong inversion (from –3.5 to –2 V). This is indicative of an unpinned Fermi level. Experimental high-frequency C-V curves agree well in slope with the theoretical curve (Fig. 1, *b*). The D_{it} distribution has essentially the same shape as the one determined in the AO case; however, the density decreases considerably throughout the entire bandgap. The value of D_{it} near the midgap is $\sim 2 \cdot 10^{11} \text{ eV}^{-1} \cdot \text{cm}^{-2}$ (78 K). Frequency dependences of G/ω -V in Fig. 1, *d* feature small peaks at a bias voltage of about –1 V. The D_{it} estimate obtained using the conductance technique is the same ($\sim 2 \cdot 10^{11} \text{ eV}^{-1} \cdot \text{cm}^{-2}$). The increase in conductance at frequencies of 1–100 kHz at reverse bias voltages from –1 to –3.5 V is associated with the response of minority carriers (holes).

The effects of C-V curves hysteresis were not examined in detail. Hysteresis magnitude ΔV at the flat-band capacitance level for high-frequency C-V curves (1 MHz) from Fig. 1 was 1.3 and 0.6 V for the structures with AO and FAO layers, respectively. With the insulator layer capacitance (C_{ox}) taken into account, the densities of trapped charge ($Q_{hyst} = \Delta V C_{ox} / q_e$) in these two cases are approximately the same and equal to $(2-3) \cdot 10^{12} \text{ cm}^{-2}$.

It is well-known that anodic (native) oxide layers on InAs consist primarily of In_2O_3 , As_2O_3 , As_2O_5 , and elemental arsenic [7].

XPS studies of the chemical composition of the FAO (7–8 nm)/InAs(001) interface revealed that the spectra of In 4*d* and As 3*d* lines feature components corresponding to the bulk of InAs [7]: In–As (17.52 eV) and As–In (40.8 eV), respectively (Fig. 2). The presence of the As–As (41.8 eV) component corresponding to elemental arsenic in the As 3*d* line spectrum should also be noted. Oxide

components of both lines may be decomposed into two constituents. The first of them (In–O (18.5 eV) and As–O (44.5 eV)) correspond to indium oxide (In_2O_3) and arsenic oxide (As_2O_3) [7]. The peak in the In 4*d* line spectrum labeled as In–OF has a 0.6 eV greater chemical shift than the In–O (In_2O_3) peak and corresponds to indium oxyfluoride ($\text{In}_x\text{O}_y\text{F}_z$), since the chemical shift between In_2O_3 and InF_3 is 1.6–2 eV [7]. A similar pattern is observed for the oxide component of the As 3*d* line, where the As–OF peak corresponds to arsenic oxyfluoride (oxidation degree 5+) [7]. Since these results agree well with the data reported earlier for InAs(111) A [7], it is fair to assume that the mechanisms of suppression of interface states due to the formation of indium and arsenic oxyfluorides are similar.

Thus, frequency (1 kHz–1 MHz) dependences of capacitance–voltage curves of Au/Ti/AO/InAs(001) and Au/Ti/FAO/InAs(001) MIS structures were analyzed, and the chemical composition of the FAO/InAs(001) interface was examined. It was demonstrated that AO fluorination results in the production of indium and arsenic oxyfluorides and has a significant positive effect on the electrophysical parameters of the oxide/InAs(001) interface. The frequency dispersions of C-V curves in enrichment and depletion are eliminated almost completely due to a reduction in the densities of border traps and interface states ($\sim 10^{11} \text{ eV}^{-1} \cdot \text{cm}^{-2}$ at 78 K).

Funding

This study was supported financially by the Russian Foundation for Basic Research as part of research project No. 20-02-00516.

Conflict of interest

The authors declare that they have no conflict of interest.

References

- [1] Q. Cheng, K. Shariar, S. Khandelwal, Y. Zeng, *Solid State Electron.*, **158**, 11 (2019). DOI: 10.1016/j.sse.2019.05.001
- [2] R. Oxland, X. Li, S.W. Chang, S.W. Wang, T. Vasen, P. Ramvall, R. Contreras-Guerrero, J. Rojas-Ramirez, M. Holland, G. Doornbos, Y.S. Chang, D.S. Macintyre, S. Thoms, R. Droopad, Y.-C. Yeo, C.H. Diaz, I.G. Thayne, M. Passlack, *IEEE Electron Dev. Lett.*, **37**, 261 (2016). DOI: 10.1109/LED.2016.2521001
- [3] J.A. del Alamo, *Nature*, **479**, 317 (2011). DOI: 10.1038/nature10677
- [4] G. D'Acunto, E. Kokkonen, P. Shayesteh, V. Boix, F. Rehman, Z. Mosahebfard, E. Lind, J. Schnadt, R. Timm, *Faraday Discuss.*, **236**, 71 (2022). DOI: 10.1039/D1FD00116G
- [5] J. Wu, E. Lind, R. Timm, M. Hjort, A. Mikkelsen, L.-E. Wernersson, *Appl. Phys. Lett.*, **100**, 132905 (2012). DOI: 10.1063/1.3698094
- [6] S. Eom, M.-W. Kong, K.-S. Seo, in *Recent advances in nanophotonics*, ed. by M. Kahrizi (IntechOpen, 2020), ch. 7. DOI: 10.5772/intechopen.92424
- [7] N.A. Valisheva, A.V. Bakulin, M.S. Aksenov, S.E. Khandarkhaeva, S.E. Kulkova, *J. Phys. Chem. C*, **121**, 20744 (2017). DOI: 10.1021/acs.jpcc.7b03757
- [8] J. Wu, E. Lind, R. Timm, M. Hjort, A. Mikkelsen, L.-E. Wernersson, *Appl. Phys. Lett.*, **100**, 132905 (2012). DOI: 10.1063/1.3698094
- [9] J. Robertson, Y. Gao, L. Lin, *J. Appl. Phys.*, **117**, 112806 (2015). DOI: 10.1063/1.4913832
- [10] M.S. Aksenov, A.Yu. Kokhanovskii, P.A. Polovodov, S.F. Devyatova, V.A. Golyashov, A.S. Kozhukhov, I.P. Prosvirin, S.E. Khandarkhaeva, A.K. Gutakovskii, N.A. Valisheva, O.E. Tereshchenko, *Appl. Phys. Lett.*, **107**, 173501 (2015). DOI: 10.1063/1.4934745
- [11] A.P. Kovchavtsev, A.V. Tsarenko, A.A. Guzev, M.S. Aksenov, V.G. Polovinkin, A.E. Nastovjak, N.A. Valisheva, *J. Appl. Phys.*, **118**, 125704 (2015). DOI: 10.1063/1.4931772
- [12] <http://www.ioffe.ru/SVA/NSM/Semicond/InAs/>
- [13] Y. Yuan, L. Wang, B. Yu, B. Shin, J. Ahn, P.C. McIntyre, P.M. Asbeck, M.J.W. Rodwell, Y. Taur, *IEEE Electron Dev. Lett.*, **32**, 485 (2011). DOI: 10.1109/LED.2011.2105241
- [14] L.M. Terman, *Solid-State Electron.*, **5**, 285 (1962). DOI: 10.1016/0038-1101(62)90111-9
- [15] E.H. Nicollian, A. Goetzberger, *Bell Syst. Techn. J.*, **46**, 1055 (1967). DOI: 10.1002/j.1538-7305.1967.tb01727.x